Nickel Nanoparticle-Doped Paper as a Bioactive Scaffold for Targeted and Robust Immobilization of Functional Proteins

Gustavo Bodelón,[†,*] Stefanos Mourdikoudis,[†] Luis Yate,[‡] Isabel Pastoriza-Santos,[†] Jorge Pérez-Juste,[†] and Luis M. Liz-Marzán[†,‡,§,*]

[†]Departamento de Química Física, Universidade de Vigo, 36310 Vigo, Spain, [‡]Bionanoplasmonics Laboratory, CIC biomaGUNE, Paseo de Miramón 182, 20009 Donostia—San Sebastián, Spain, and [§]Ikerbasque, Basque Foundation for Science, 48011 Bilbao, Spain

ABSTRACT Cellulose-based materials are widely used in analytical chemistry as platforms for chromatographic and immunodiagnostic techniques. Due to its countless advantages (*e.g.*, mechanical properties, three-dimensional structure, large surface to volume area, biocompatibility and biodegradability, and high industrial availability), paper has been rediscovered as a valuable substrate for sensors. Polymeric materials such as cellulosic paper present high protein capture ability, resulting in a large increase of detection signal and improved assay sensitivity. However, cellulose is a rather nonreactive material for direct chemical coupling. Aiming at developing an efficient method for controlled conjugation of cellulose-based materials with proteins, we devised and fabricated a hybrid scaffold based on the adsorption and *in situ* self-assembly of surface-oxidized Ni nanoparticles on filter paper, which serve as "docking sites" for the selective immobilization of proteins containing polyhistidine tags (His-tag). We demonstrate that the interaction between the nickel substrate and the His-tagged protein G is remarkably resilient toward chemicals at concentrations that quickly disrupt standard Ni-NTA and Ni-IDA complexes, so that this system can be used for applications in which a robust attachment is desired. The bioconjugation with His-tagged protein G allowed the binding of anti-*Salmonella* antibodies that mediated the immuno-capture of live and motile *Salmonella* bacteria. The versatility and biocompatibility of the nickel substrate were further demonstrated by enzymatic reactions.

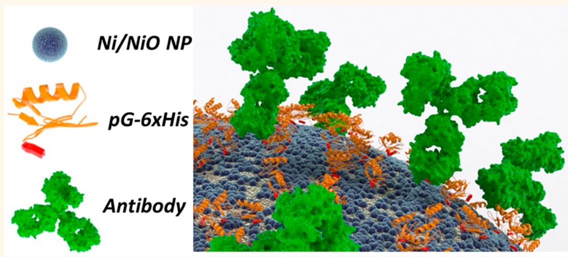

KEYWORDS: nickel nanoparticles · filter paper · bioconjugation · polyhistidine tag · protein G · immuno-capture · *Salmonella* · enzyme immobilization

The development of novel materials with improved properties for protein analysis, diagnostics, therapeutics, or drug screening is at the leading edge of modern biological sciences, medicine, and biotechnology.[1,2] The success of these technologies requires the immobilization of proteins (*e.g.*, enzymes, antibodies) on solid surfaces by a simple and scalable process, in a way that their biological function is maintained. Whereas the immobilization on planar surfaces yields limited protein density, polymeric materials such as cellulose paper, bearing a three-dimensional structure, present higher protein capture ability, which may result in a large increase of signal detection and improved assay sensitivity.[3] In contrast to other types of polymeric substrates, the low-cost, simplicity, high strength-to-weight ratio, inherent resource renewability, and friendliness for printing, coating, or impregnation have motivated the use of cellulose-based materials (*e.g.*, filter paper) to perform analytical functions[4−6] and as potential lab-on-a-chip (LOC) devices.[7]

The immobilization of proteins in paper-based sensing devices has been carried out mainly by physical adsorption on charged surfaces and covalent conjugation. Physisorption is the simplest route to attach proteins to cellulose. However, this approach often inactivates or lowers the protein biological activity, there is no control over protein orientation, and in most cases the biomolecules are not firmly anchored

* Address correspondence to gbodelon@uvigo.es; llizmarzan@cicbiomagune.es.

Received for review March 26, 2014 and accepted May 8, 2014.

Published online May 08, 2014
10.1021/nn5016665

and can thus be easily washed off. Additionally, cellulose offers relatively few functional groups for direct chemical coupling. These drawbacks have motivated the development of sophisticated conjugation chemistries, which usually are not site-specific and have the potential to cause inactivation of the protein because attachment occurs either randomly or through multiple points.[4,5] An alternative strategy involves the use of a cellulose-binding module (CBM), which consists of a small peptide with high affinity toward cellulose that is genetically fused to the protein of interest.[8] Despite all these efforts, the reported biorecognition assays usually lack sensitivity, and new strategies are highly demanded for implementation of reliable, robust, and sensitive methods that allow the functionalization of paper with delicate and complex macromolecules such as proteins.[9]

Nanoparticles (NPs) with distinctive properties are at the forefront of research due to their numerous applications. It is well established that the porous structure and hydrophilic surface of paper provides it with the ability to absorb NP colloids through capillary forces, ultimately leading to high NP loadings upon drying. Therefore, filter paper has been extensively used as an inert support for NP adsorption to produce devices with outstanding optical, antibacterial, catalytic, or plasmonic performances.[6,9] Moreover, it has been reported that, compared with biomacromolecules, it is easier to concentrate colloidal particles onto the surface of porous paper.[5]

With the aim of developing an efficient method toward controlled biofunctionalization of paper-based materials with proteins, we devised and fabricated a hybrid scaffold based on the adsorption and *in situ* self-assembly of surface-oxidized nickel NPs on filter paper. The assembled NPs serve as "docking sites" for the selective immobilization of proteins containing polyhistidine tags (His-tag). The affinity interaction between transition metal ions (Ni^{2+}, Co^{2+}, Cu^{2+}, or Zn^{2+}) and histidine has been used as a site-specific, noncovalent method for the purification and immobilization of recombinant proteins bearing three to 10 consecutive histidine amino acids at their amino- or carboxy-terminus.[10,11] In this approach, typically Ni^{2+} ions (or other divalent ions such as Co^{2+}, Cu^{2+}, or Zn^{2+}) are covalently linked to a matrix *via* nitrilotriacetic acid (NTA) or iminodiacetic acid (IDA) and engage coordinative bonds with the imidazolic rings of the polyhistidine, without interfering with the polyhistidine-tagged structure or function. Importantly, this interaction is reversible, and upon treatment with low concentrations of competitive ligands (imidazole), metal chelators (EDTA), or reductants (DTT) or protonation of histidine groups (pK_a = 6.0), the polyhistidine-tagged protein can be released from the matrix and purified. Due to the specificity of this interaction, its use has been extended to applications involving protein–protein interactions such as ELISA,[12] microarrays,[13] or SPR biosensors,[14] in which proteins need to be immobilized on surfaces while keeping a biologically active conformation. However, a severe limitation of this approach is the relatively low affinity (in the micromolar range) between the His-tag and the transition metal ions chelated by commonly used ligands (*e.g.*, NTA, IDA). Ni-NTA and Ni-IDA are kinetically labile complexes that can be easily disrupted by DTT or EDTA at concentrations often found in many buffers for protein chemistry.[10,11] This hampers their use in certain applications in which a permanent immobilization is required. In an elegant study, Wegner and Spatz reported a strategy to generate a permanent interaction between a polyhistidine-tagged GFP and NTA-Co^{3+} beads through oxidation of NTA-Co^{2+} to Co^{3+}.[15] This interaction was completely inert toward ligand exchange with EDTA (25 mM) and imidazole (250 mM) in combination with DTT (1 mM) or TCEP (1 mM). However, as the authors stated, the requirement of an oxidizing agent to form Co^{3+} limits the applications of this approach to proteins that are not sensitive to oxidation.[15]

Besides Ni-NTA or Ni-IDA systems, nickel oxide surfaces[16,17] and colloidal dispersions of Ni NPs have been reported to bind His-tagged proteins.[18−20] For example, Lee *et al*. used Ni nanorods with gold end blocks that acted as magnetic nanosized affinity templates with large surface area for separation of His-tagged from non-His-tagged proteins by applying an external magnetic field.[18] Hyeon and co-workers employed Ni/NiO core/shell NPs as well as magnetic nanocomposite spheres decorated with NiO NPs for the selective binding and magnetic separation of His-tagged proteins.[19,20]

In this context, we employed oxidized nickel NPs for implementing a simple yet efficient strategy for the robust functionalization of filter paper with His-tagged protein G, an antibody-binding protein.[21] We demonstrate that the interaction between the oxidized Ni composite and the polyhistidine-tagged protein is significantly more stable and chemically inert toward the action of competitive ligands (imidazole), reducing agents (DTT and TCEP), and metal chelators (EDTA) than the widely used Ni-NTA and Ni-IDA systems. The immobilization of functional His-tagged protein G to this substrate provides efficient binding sites for antibodies, thereby rendering a homogeneous coverage of this polymeric structure. Finally, we applied the cellulose–nickel NP composite material functionalized with His-tagged protein G as a platform for immunocapturing motile *Salmonella enterica* bacteria, as well as for performing enzymatic reactions, thus demonstrating its biocompatibility and versatility.

RESULTS AND DISCUSSION

The process for fabrication of the hybrid scaffold is schematically depicted in Scheme 1 and comprises

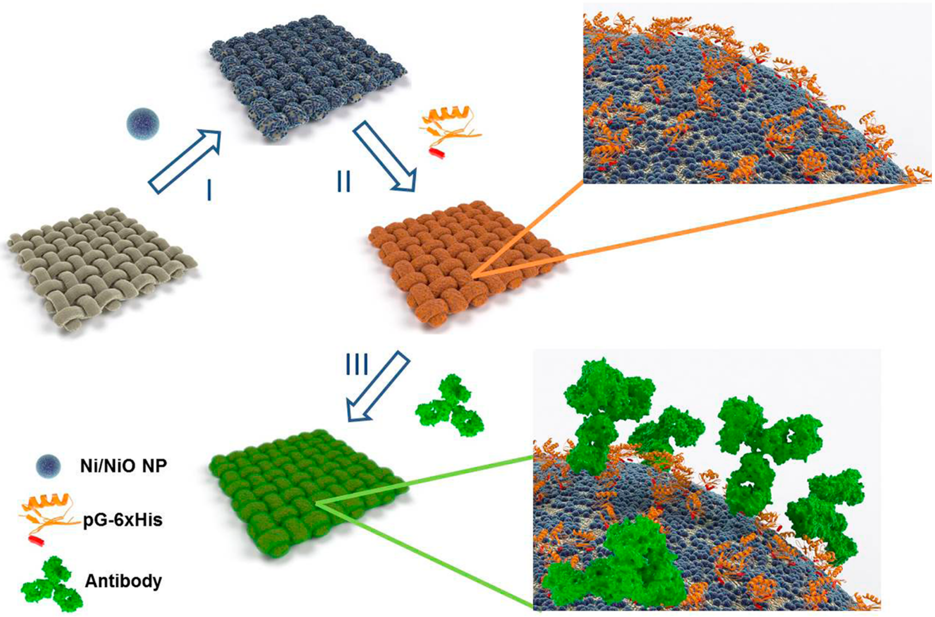

Scheme 1. Schematic representation of the bioactive scaffold preparation: (I) adsorption of nickel NPs on filter paper, (II) targeted immobilization of the polyhistidine-tagged protein G (pG-6xHis), and (III) protein G-mediated capture of antibodies. Protein G is represented by the protein G B1 domain (PDB: 1GB1, orange) bearing a 6xHis at its C-terminus (red). The antibody is an IgG2a immunoglobulin (PDB: 1IGT, green). Both proteins were modeled with PyMOL.

three main steps. First, nickel NPs are adsorbed on the polymeric cellulose acetate substrate (step I, Scheme 1) by immersion and drying. Subsequently, His-tagged protein G is selectively immobilized on the surface of the adsorbed nickel nanoparticles (step II, Scheme 1). Finally, the oriented immobilization of antibodies occurs through protein G binding (step III, Scheme 1).

The preparation of the substrate for protein immobilization involves the combination of Ni NPs stabilized by oleylamine (OAm) and trioctylphosphine (TOP), with cellulose acetate filter paper. The choice of filter paper as a support was based not only on its low cost, renewable character, easy handling, and metal recovery, as well as high surface area (due to its microfiber composition), but also on its ability to wick fluids *via* capillary action and strong adhesion to a variety of materials.[22,23] On the other hand, metal NPs stabilized by fatty acids such as oleic acid or oleylamine have been demonstrated to readily form one-, two-, and even three-dimensional superlattice assemblies.[24−26] OAm/TOP-stabilized Ni NPs with an average diameter of 3.5 ± 0.6 nm (Figures 1A and S1, Supporting Information) were prepared as previously reported (see Experimental Section for details).[27] Prior to assembly on paper, the as-prepared NPs were washed by precipitation with ethanol to ensure removal of excess OAm and TOP, the supernatant was discarded, and the precipitate was redispersed in chloroform. Loading of Ni NPs on cellulose paper was carried out by simply dipping a paper strip (typically 0.4 cm $\times$ 0.4 cm, Figure 1B) in the Ni NP dispersion in chloroform for 5−10 s. Subsequently, the paper strip was pulled out and blow-dried for typically 5 min. Such an impregnation process can be repeated several times to maximize NP loading. The Ni-loaded paper strips were then dried overnight at 60 °C and washed in water, ethanol, and chloroform to remove unbound NPs and impurities (such as OAm and TOP excess). It is important to point out that no desorption of Ni NPs from the paper substrate was observed after drying, even when soaked in chloroform, demonstrating an extremely tight adsorption of the NPs to the substrate. The loading process relies on a combination of hydrophobic and van der Waals interactions, which promote the formation of organized NP superlattices upon solvent evaporation, with considerable mechanical robustness.[28]

The Ni NPs-doped paper support was characterized by scanning electron microscopy (SEM), as shown in Figure 1C. Unfortunately, the small particle size, together with the organic nature of the substrate, did not allow us to distinguish the individual NPs. However, energy-dispersive X-ray spectroscopy (EDX) analysis demonstrates the presence of nickel in the modified paper, as compared to nondoped paper (Figure S2, Supporting Information). To demonstrate the dense packing of the NPs on the paper surface, it was embedded in an epoxy resin, which allowed the preparation of ultrathin slices using an ultramicrotome (see Experimental Section). Figure S3 (Supporting Information) shows a representative TEM image of the cross section of a cellulose fiber, in which the close packing of the particles on the fiber surface can be clearly visualized. Additionally, we analyzed in detail the chemical nature of the NP surface, which was

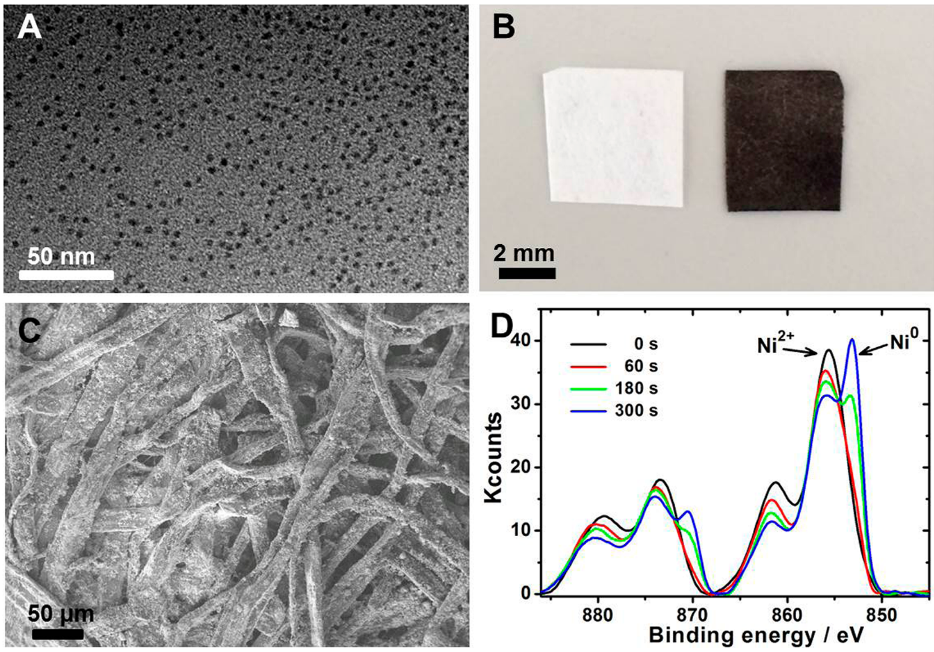

Figure 1. (A) Transmission electron microscopy image of Ni NPs. (B) Photograph of the filter paper before and after Ni doping. (C) Scanning electron microscopy image of cellulose fibers doped with Ni NPs. (D) High-resolution Ni(2p) XPS depth profiling of the paper-supported Ni NPs.

essential from the applicability point of view. X-ray photoelectron spectroscopy (XPS) was thus used to investigate the oxidation state of the Ni NPs. Figure 1D displays the XPS Ni(2p) core level peaks from the Ni-doped filter paper. The spectrum shows the characteristic Ni $2p_{3/2}$ and $2p_{1/2}$ peaks and their corresponding shake-up satellite peaks, characteristic of Ni^{2+} ions (Figure S4, Supporting Information). Shown in the same figure is the deconvolution analysis of the Ni(2p) region (840–900 eV), revealing the presence of a small peak at around 852.92 eV attributed to Ni^0, which thus seems to coexist with Ni^{2+} in the sample.[29] Further information about the structure and composition of the Ni NPs supported on the cellulose paper was obtained from a depth-profiling experiment, in which the sample was gradually etched by ion-beam irradiation. However, we need to be cautious during interpretation, as the measurements were performed on nanoparticles deposited on a cellulose substrate, and thus we probe a large amount of particles at the same time that are not necessarily at the same height on the substrate. Therefore, different sections at increasing depths within the particles were gradually probed by successive XPS measurements. High-resolution XPS spectra (in the region of 840–900 eV) at different etching times are shown in Figure 1D, clearly showing that as deeper sections are probed in the particles, the Ni^0 peak gradually shows up while the Ni^{2+} peak intensity decreases. This is an indication of the core–shell Ni/NiO structure of the NPs. Although it has been reported that Ni^{2+} can be reduced into Ni^0 during etching with Ar^+ ions,[29] the presence of a Ni^0 peak in the sample prior to etching, at approximately the same peak position and with FWHM in the same order (see Figure S4, Supporting Information), validates the analysis. Peak deconvolution at different etching times allowed us to indentify the contributions from both Ni^{2+} and Ni^0 species (see Figure S4, Supporting Information), showing that the percentage of Ni^0 increased from 2.6% to 46.6% during etching (Table S1, Supporting Information) and providing further confirmation of the Ni/NiO core–shell structure of the NPs on the paper substrate.

A binding assay was performed to evaluate the performance of the nickel substrate for selective immobilization of polyhistidine-tagged proteins. A piece of nickel NP-doped paper (4 mm $\times$ 4 mm) was incubated with either protein G tagged with 6xHis at its C-terminus (pG-6xHis) or protein G without the polyhistidine tag (pG), both in phosphate-buffered saline, PBS (see the Experimental Section for details). After collecting the unbound protein fraction, the nickel paper was incubated with imidazole (250 mM) for 5 min, which is a standard process for eluting His-tagged proteins from Ni^{2+}-NTA beads,[10,11] and then boiled in a buffer containing sodium dodecyl sulfate (SDS) and beta-mercaptoethanol (β-ME) to release any protein that remained bound. Subsequently, the eluted fractions were analyzed by polyacrylamide gel electrophoresis (SDS-PAGE) and visualized by protein staining (see Experimental Section). As shown in Figure 2A, the protein G lacking polyhistidines did not bind to the nickel substrate and was detected in the unbound fraction (U, lane 2). On the contrary, the pG-6xHis did

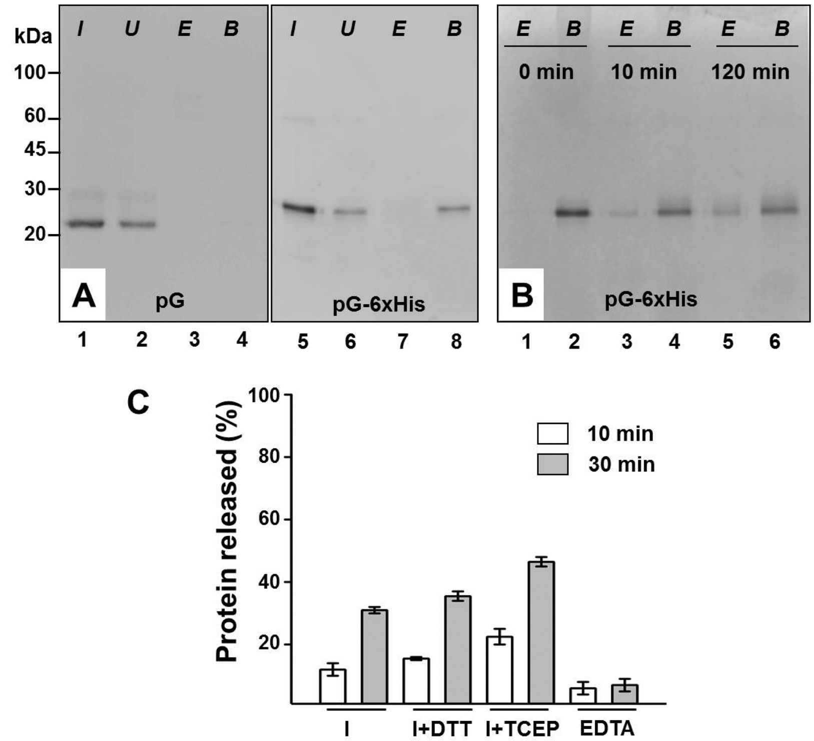

Figure 2. (A) SDS-PAGE analysis of protein G (without polyhistidines, pG, and with polyhistidines, pG-6xHis) eluted from nickel substrates: (*I*) Input, (*U*) not bound, (*E*) elution with 250 mM imidazole, (*B*) elution by boiling. (B) SDS-PAGE analysis of the pG-6xHis elution with 1 M imidazole (*E*) and by boiling (*B*) at the indicated times. (C) Quantification of pG-6xHis elution with 1 M imidazole (I), 1 M imidazole + 1 mM DTT (I+DTT), 1 M imidazole + 1 mM TCEP (I+TCEP), and 50 mM EDTA (EDTA).

bind to the Ni substrate and was equally distributed between the unbound (U, lane 6) and bound fractions (B, lane 8). These results demonstrate that the polyhistidine tag was involved in the binding of protein G to the nickel NP-doped paper. The binding capacity of the substrate was 0.15 $\mu g/mm^2$, as calculated by densitometric analysis measuring the intensities of the protein bands in the SDS-PAGE gels with commercially available software as indicated in the Experimental Section. Interestingly, treatment of the protein G-functionalized nickel substrate with 250 mM imidazole did not release the pG-6xHis protein (Figure 2A, lane 7), and the protein was eluted off the substrate only by boiling (lane 8). We further investigated the immobilization extent of the histidine-tagged protein G to the nickel substrate by a treatment with 1 M imidazole for 2 h. At selected times, the eluted fractions obtained after both imidazole and boiling treatments were collected and subjected to SDS-PAGE electrophoresis. As shown in Figure 2B, after 10 min of 1 M imidazole treatment the protein was barely detectable in the gel (lane 3), whereas most of it was present in the boiled fraction (lane 4). Unexpectedly, when the incubation time was extended to 120 min, although the amount of imidazole-eluted protein slightly increased (lane 5), most of the protein remained attached to the nickel substrate (lane 6). The densitometry analysis performed in polyacrylamide gels to quantify the amount of protein released with 1 M imidazole at various time points (Figure S5, Supporting Information) revealed that less than 20% and a maximum of approximately 39% of the total protein was released at 10 and 120 min, respectively, and that most of the elution took place after 30 min. Altogether, these data indicate that in contrast to the binding of polyhistidines to Ni-NTA or Ni-IDA, which can be easily disrupted by low imidazole concentrations (50−250 mM),[10,11] the interaction between the pG-6xHis and the NiO is highly resilient. This is in agreement with the results by Mirkin and coworkers, who reported a strong binding interaction between a histidine-tagged ink and a nickel oxide substrate prepared by thermal evaporation of Ni (30 nm) on Si(100) wafers.[17] Interestingly, Lee *et al.*[19] and Kim *et al.*,[20] exploring the use of magnetic Ni NPs for the reversible binding of polyhistidine-tagged GFP, had to employ an even higher imidazole concentration of 1.4 M to release 70% of the protein from their NPs after 30-minute incubations.

To further characterize the interaction between the polyhistidine-tagged protein and the nickel substrate, we analyzed its stability toward the action of two reducing agents (1 mM DTT and 1 mM TCEP) combined with 1 M imidazole and 25 mM EDTA, a strong chelator that, at concentrations above 1 mM, usually reduces and strips nickel ions from commercial Ni-NTA and Ni-IDA resins. The densitometric analysis of Figure 2C shows the percentage of pG-6xHis eluted from the paper after either 10 or 30 min incubation with the

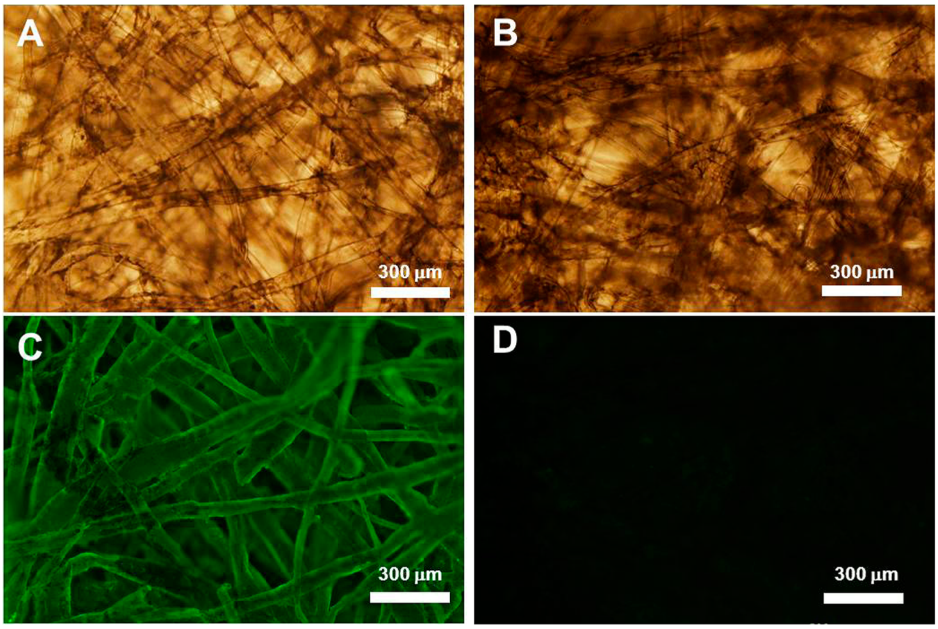

Figure 3. Bright field (A, B) and fluorescence (C, D) microscopy images of nickel substrates incubated with pG-6xHis (A, C) or with pG (B, D) and stained with a goat anti-mouse IgG-FITC.

indicated treatments. DTT plus imidazole presented values of protein release similar to those obtained with imidazole alone, indicating that DTT does not affect the stability of the complex. The incubation with TCEP plus imidazole slightly increased the percentage of eluted protein to approximately 20% after incubation for 30 min, as compared with imidazole alone. Strikingly, the treatment with EDTA was found not to affect the interaction, since it did not cause the release of pG-6xHis at significant levels. Again, we find that Ni NP-doped paper and pG-6xHis form a stable complex that is capable of opposing ligand exchange with imidazole, chelation, and reduction under conditions that usually disrupt interactions between transition metal ions, metal chelators, and polyhistidines. The interaction was affected upon a long incubation time with 1 M imidazole and slightly enhanced by 1 mM TCEP, a more stable and effective reducing agent than DTT.[30]

It is however important to verify whether the immobilization of pG-6xHis to the nickel substrate affects the function of the protein. Protein G is an immunoglobulin-binding protein, and, as such, it is commonly used for purifying antibodies (IgGs) through binding to the Fab and Fc regions of most IgG subtypes.[21,31] This interaction leaves the antigen-binding site of the antibody available for antigen−antibody interactions, which has rendered protein G a useful tool for the oriented immobilization of antibodies onto solid surfaces.[32] Assessment of the functional activity of immobilized pG-6xHis was carried out using a goat anti-mouse antibody labeled with a standard fluorophore (IgG-FITC). We found that, whereas the nickel substrate functionalized with pG-6xHis (Figure 3A,C) was indeed stained with the fluorescent antibody, the control substrate (nickel NP-doped paper incubated with pG lacking polyhistidine tag) (Figure 3B,D) was not stained. This result confirms the binding of protein G to the nickel substrate *via* the polyhistidine tag in a functional conformation, thereby maintaining its biological activity. Importantly, the fluorescence from the FITC fluorophore linked to the antibody was homogeneously distributed over all the fibers in the nickel paper substrate (Figure 3C and Figure S6, Supporting Information) mainly due to the targeted binding of pG-6xHis.

Once the functional activity of the Ni-pG-6xHis substrate was confirmed, we explored its use in two different applications, namely, the capture of motile *Salmonella* bacteria, a causative agent of food poisoning all over the world,[33] and reactions catalyzed by immobilized enzymes.

Bacteria are often used as cellular biosensors for monitoring biological processes such as quorum sensing,[34] for detection of environmental pollutants,[35] or for industrial applications.[36] The ability to control the adhesion of bacteria on a surface provides a unique opportunity to obtain reusable bacteria-based biosensors, as well as allowing the interrogation of immobilized bacteria, either at the single-cell level or in spatially oriented bacteria populations. Also, efficient and reliable immobilization methods that enable the selective separation and concentration of a specific microorganism from a mixed population have important applications in biomedicine or in the food industry. On the other hand, techniques such as the polymerase chain reaction (PCR) are rapid, reliable, and highly sensitive for the identification of microbial pathogens.[37] However, the presence of PCR inhibitors

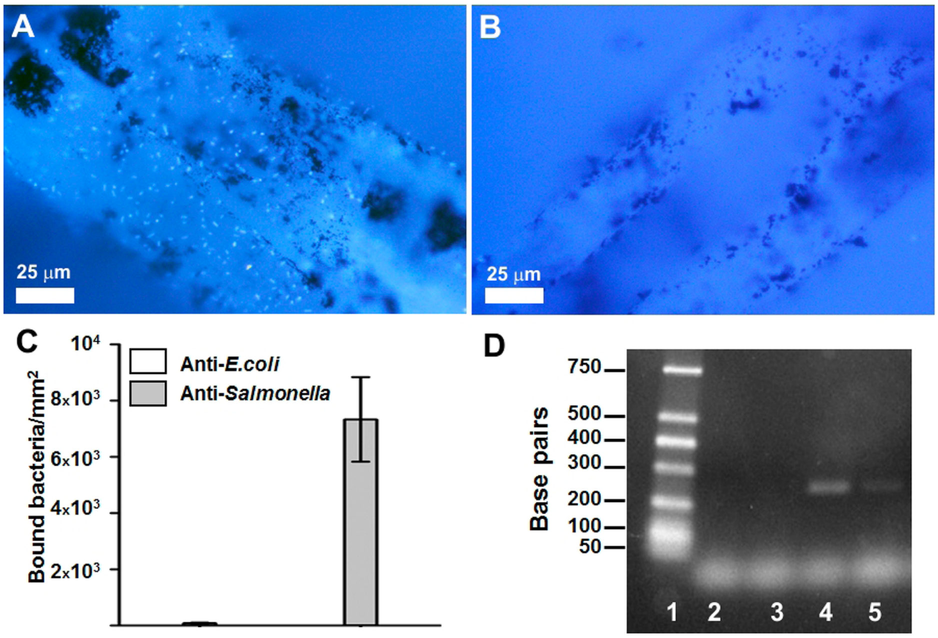

Figure 4. (A, B) Fluorescence images showing the immobilization of *Salmonella* bacteria onto Ni-pG-6xHis substrate functionalized with anti-*Salmonella* (A) or anti-*E. coli* (B) antibodies. (C) Quantification of bound bacteria to Ni-pG-6xHis substrate functionalized with anti-*E. coli* (white) or anti-*Salmonella* (gray) antibodies. (D) PCR amplification of *invA* amplicon by PCR.

or contaminant DNA fragments in the sample may negatively affect the results.[38,39] Therefore, separation and concentration of bacteria with suitable substrates could improve the sensitivity of the PCR methods available for detection. The immobilization of bacteria onto a solid support mediated by an antigen−antibody interaction is highly specific and allows the selection of a particular bacterial species from a mixed culture.[40] This approach requires attachment of the antibody to the surface, and although chemical conjugations are usually employed,[41−43] these are often technically complex and may lead to the decrease of the antibody biological activity or even to its complete inactivation. Since we have demonstrated that the Ni-pG-6xHis substrate can efficiently capture antibodies, we employed it as a platform for antibody-mediated immobilization of live and motile *S. enterica*. To this end, we functionalized Ni-pG-6xHis substrates with either a specific antibody against *S. enterica* or a control antibody against *Escherichia coli*. Upon incubation with a bacterial suspension of *Salmonella*, previously stained with DAPI (4′,6-diamidino-2-phenylindole), nonadherent bacteria were removed through several washes with PBS, and the presence of bound bacteria was analyzed by fluorescence microscopy. As shown in Figure 4, the substrate bearing anti-*Salmonella* antibodies captured more bacteria (Figure 4A) than the control substrate functionalized with anti-*Escherichia coli* antibodies (Figure 4B). The quantification of bound bacteria, performed in a single focal plane, as described in the Experimental Section, showed a difference of at least 3 orders of magnitude between them (Figure 4C). On the other hand, imaging at different focal planes within the same area clearly reveals the presence of numerous *Salmonella* bacteria surrounding the same fiber (Figure S7, Supporting Information). Hence, if we take into account that the quantification of bacteria was performed in a single focal plane, the number of bound bacteria per mm^2 is expected to be much higher than the values provided in Figure 4C. Therefore, the pG-6xHis-mediated oriented display of anti-*Salmonella* antibodies permits the immobilization of these motile bacteria, possibly by increasing the avidity by the substrate. Also, the inert nature of the nickel substrate resulted in low nonspecific binding of bacteria and therefore avoided the need for passivation of the surface, which is usually required in other approaches to avoid nonspecific adsorption.[40,41,43] The presence of immuno-captured bacteria was assessed by the polymerase chain reaction. To this end, Ni-pG-6xHis substrates bearing antibodies against either *Salmonella* or *E. coli* were incubated for 30 min with 10^5 CFUs of *Salmonella* bacteria in PBS. After rinsing unbound bacteria with PBS, the anti-*Salmonella* or anti-*E. coli* Ni-pG-6xHis substrates, immersed in 50 μL of PBS, were heated for 5 min at 95 °C to lyse the bacterial cells. Subsequently, two aliquots of 1 and 5 μL were transferred to a PCR mixture containing a pair of specific primers for the *invA* gene,[44] which is recognized as an international standard for detection of *Salmonella* serovars.[45] As shown in Figure 4D, PCR products of the expected size (244 bp) were amplified from the anti-*Salmonella* Ni-pG-6xHis substrate using both 5 and 1 μL (lanes 4 and 5, respectively) but not from the control substrate functionalized with anti-*E. coli* antibodies (lanes 2 and 3). This indicates that the *invA* amplicon was specifically amplified from immunocaptured *Salmonella* bacteria. Since the nickel substrate was not inhibitory to the PCR reaction, it could be used as an analytical platform for the specific concentration of bacteria from food or environmental samples with the aim to facilitate or improve bacterial detection by PCR.

Finally, we investigated the performance of the nickel substrate toward enzymatic reactions. To this end, an antibody-conjugated horseradish peroxidase enzyme (HRP), which catalyzes the oxidative chemiluminescent reaction of luminol (emission centered at 425 nm), was incubated for 5 min with Ni-pG-6xHis. A nickel substrate lacking pG-6xHis was used as control. After washing the unbound antibody with PBS, the Ni NP-doped paper was incubated with the HRP substrate, and the enzymatic reaction was allowed to proceed for 1 min. Next, the chemiluminescence signal was measured with an ELISA plate reader. As shown in Figure 5A, the enzymatic reaction was catalyzed by the Ni-pG-6xHis substrate but not by the control substrate. Immobilized biocatalysts offer significant advantages over their soluble counterparts such as easier separation of the biocatalysts from the product, allowing its continuous use, and reduced cost.[46,47] Therefore, we tested the reusability of the HRP-functionalized Ni-pG-6xHis substrate. To this end, the Ni-pG-6xHis substrate was functionalized with IgG-HRP as describe above, washed with PBS, and incubated with the peroxidase chemiluminescent HRP substrate, and the production of light was monitored with an ELISA plate reader. After 15 min the substrate was washed with PBS and measured to confirm that no enzymatic product remained adsorbed, and 15 min later it was incubated again with the HRP substrate and monitored for light production. As illustrated in Figure 5B, the enzymatic reaction was performed four times without significant loss of enzymatic activity. We thus conclude that the nickel substrate not only can accommodate enzymatic reactions but also allows repeated use of the biocatalyst. Therefore, the use of this substrate as a novel platform for the immobilization of polyhistidine-tagged enzymes constitutes a promising approach toward industrial and biotechnological applications.

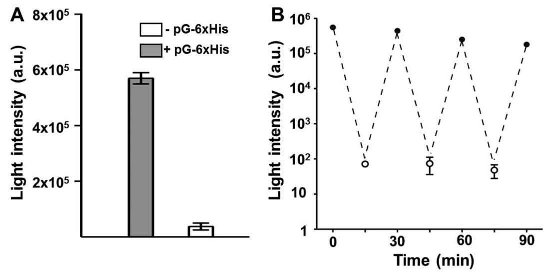

Figure 5. (A) Enzymatic reactions catalyzed by an antibody-conjugated horseradish peroxidase (IgG-HRP) on nickel substrates that were functionalized with pG-6xHis (gray bar) or not functionalized (white bar). (B) Reutilization of Ni-pG-6xHis substrate. The enzymatic reactions catalyzed by an antibody-conjugated horseradish peroxidase (IgG-HRP) were performed in the presence (black circles) or absence (empty circles) of the HRP substrate.

CONCLUSIONS

We have demonstrated the fabrication of bioactive hybrid scaffolds with large surface area through the adsorption and self-assembly of oxidized nickel NPs on cellulose paper. The NPs mediated the oriented binding of functional His-tagged protein G to the substrate, as demonstrated by the subsequent binding of fluorescent antibodies, which were homogeneously distributed over the composite substrate. Furthermore, the interaction between the nickel substrate and the polyhistidine-tagged protein is highly resilient and chemically inert toward chemicals at concentrations that quickly disrupt standard Ni-NTA and Ni-IDA complexes, thereby demonstrating that this platform is of interest for those applications in which a robust attachment is required. The targeted bioconjugation of His-tagged protein G allowed the oriented binding of anti-*Salmonella* antibodies that allowed the immobilization of live and motile *Salmonella* bacteria on the substrate. The versatility and biocompatibility of the nickel substrate were further demonstrated by means of two different enzymatic reactions performed by a polymerase to synthesize DNA or a peroxidase to produce light. To our knowledge, this is the first report describing the use of metallic NPs as a tool for the functionalization of a cellulose-based substrate with proteins. The simplicity of the strategy described in this work paves the way for the use of other types of metallic NPs as docking sites for biomolecules (*e.g.*, paper doped with Au or Ag NPs could bind proteins and DNA through thiol chemistry). Finally, this strategy for NP-mediated protein immobilization on paper should be compatible with spotting for multiplex format, automated coating, and/or printing methods, thus facilitating potential and inexpensive large-scale applications.

EXPERIMENTAL SECTION

Materials. All chemical reagents were used as received without further purification. Nickel acetylacetonate (95%), oleylamine (70%, technical grade), trioctylphosphine (90%, technical grade), and methanol (99.6%) were obtained from Sigma-Aldrich.

Synthesis of Ni Nanoparticles. Ni NPs were synthesized by a slight modification and a limited scale-up of a previously published protocol.[27] Briefly, in a Schlenk flask containing 17 mL of oleylamine, 4.6 mmol of $Ni(acac)_2$ was introduced, and the mixture was heated to 100 °C under Ar flow. In a separate three-neck flask, 11.5 mL of trioctylphosphine was degassed with successive Ar-vacuum cycles, followed by heating at 100 °C under Ar for 10 min and then at 220 °C for another 10 min. At this point the three-neck flask was opened to introduce the $Ni(acac)_2$−OAm mixture, and Ar flow was applied again, followed by heating at 220 °C for 30 min. The final black solution was allowed to cool before precipitation with excess ethanol (8000 rpm, 30 min). The solid product was then washed with a mixture of hexane and excess ethanol, followed by storage in chloroform to obtain a stable colloidal solution.

Fabrication of Ni NP-Doped Cellulose Substrate. Small square pieces of cellulose filter paper (0.4 cm × 0.4 cm) were repeatedly dipped in a colloidal solution of Ni NPs in chloroform. After each dip the paper was allowed to dry in air to ensure continuous loading of NPs onto the cellulose fibers. After four dips, the material was dried overnight in an oven at 60 °C. The substrates were subsequently dipped for 10 min in water, ethanol, and chloroform to remove any loosely adsorbed residues. Finally, the Ni-doped paper strips were dried for 3 h at 60 °C.

Characterization. TEM images were acquired using a JEOL 1010 microscope operating at 100 kV. For the observation of Ni NPs embedded in cellulose filter papers, small pieces of approximately 0.5 cm × 0.1 cm were inserted in epoxy resin at 60 °C for 48 h. The obtained solid material was cut into very fine segments (70−75 nm thick) using a Leica Reichert Ultracut ultramicrotome, which were then entrapped in Formvar (0.25%) carbon-coated Cu grids for TEM imaging. Scanning electron microscopy was carried out in a JEOL JSM 6700F FEG microscope operating at an acceleration voltage of 15 kV and with a secondary-electron detector. XPS experiments were performed in a SPECS Sage HR 100 spectrometer with a nonmonochromatic X-ray source (Mg Kα line of 1253.6 eV energy and 250 W and calibrated using the $3d_{5/2}$ line of Ag with a full width at half-maximum (FWHM) of 1.1 eV). An electron flood gun was used to compensate for charging during XPS data acquisition. The selected resolution was 30 eV of pass energy and 0.5 eV/step for the general survey spectra and 15 eV of pass energy and 0.15 eV/step for the detailed spectrum. All measurements were made in an ultra-high-vacuum chamber at a pressure around 10^{-8} mbar. Etching was performed with a 3 kV Ar^+ beam.

Immobilization of Protein G, Chemical Reactivity, and SDS-Polyacrylamide Gel Electrophoresis. The nickel NP-doped paper (approximately 4 × 4 mm^2) was immersed in methanol, washed in distilled water, and stored in PBS until use. Next, the substrate was incubated with a solution of PBS−BSA (10 mg/mL) for 10 min and immersed in PBS (50 μL) containing 5 μg of 6xHis-tagged protein G (pG-6xHis, Genscript, Z02007) or protein G lacking the 6xHis epitope (pG, ProSpec, pro-402). After 30 min incubation, the PBS containing unbound protein was removed and kept for SDS-PAGE analysis. The paper substrate was then rinsed five times with PBS and immersed in 50 μL of PBS or in 50 μL of PBS containing the following reagents: imidazole, imidazole plus TCEP, imidazole plus DTT, or EDTA at the concentrations indicated in the Results section. Prior to SDS-PAGE, 10 μL of SDS-PAGE sample buffer (6×) was added to each sample and heated at 100 °C for 5 min. The SDS-PAGE sample buffer (1×) contains 60 mM Tris-HCl (pH 6.8), 2% (wt/v) SDS, 5 mM EDTA, 5% (v/v) glycerol, 0.005% (wt/v) bromophenol blue, and 1% (v/v) 2-β-mercaptoethanol. Electrophoresis was performed in SDS-polyacrylamide gels (12%) with a Miniprotean III electrophoresis system (Bio-Rad). After electrophoresis, the protein gels were stained with Coomassie brilliant blue R250 and scanned in a gel documentation system (Gel Doc EZ Imager, Bio-Rad). The quantification of protein bands in the SDS-PAGE gels was performed by densitometry using the Image lab software (Bio-Rad).

Fluorescence Staining of Protein G. Protein G (5 μg) was immobilized in the nickel substrate as described in the above paragraph and incubated with anti-mouse IgG-FITC (Sigma; 1:50) in 50 μL of PBS−BSA (10 mg/mL) for 5 min and rinsed 5-fold with PBS. Next, the substrate was deposited on a glass slide on top of a drop of ProLong gold antifade reagent (Invitrogen), sealed with a coverslip, and visualized with a fluorescence microscope (Olympus BX51). The Olympus DP controller software was used for image acquisition.

Immuno-capture of *Salmonella* Bacteria. A single colony of *Salmonella enterica* (ATCC 4931) was grown at 30 °C in LB broth for 18 h. The culture was harvested by centrifugation (4000*g*, 5 min), resuspended in PBS, centrifuged again, and redispersed in PBS. The cell density was adjusted to OD_{600} = 1 (1 OD_{600} = 1 × 10^8 cells/mL) with PBS. Nickel substrates with or without pG-6xHis (5 μg) were incubated with anti-*Salmonella* (Innaves Biotech; 1:100) or anti-*E. coli* (Biodesign 1:100) antibodies in 50 μL of PBS−BSA (10 mg/mL) for 10 min and rinsed 5-fold with PBS. Subsequently, the substrate was immersed in 200 μL of PBS containing the bacterial CFUs indicated in the Results section and incubated for 30 min. After removing unbound bacteria with five washes of PBS, bound bacteria were stained with DAPI (5 μg/mL). The substrate was then rinsed with PBS, deposited on a glass slide on top of a drop of ProLong gold antifade reagent (Invitrogen), sealed with a coverslip, and visualized with a fluorescence microscope (Olympus BX51). Quantification of bound bacteria to the nickel substrate was performed by counting bacterial cells in five images (40× magnification) obtained from three independent studies.

PCR Amplification of *Salmonella invA* Gene. The oligonucleotides INVA-1 (ACAGTGCTCGTTTACGACCTGAAT) and INVA-2 (AGACGACTGGTACTGAT-CGATAAT)[44] were synthesized by Sigma Genosys, and PCR was performed with Taq DNA polymerase (New England Biolabs), according to the manufacturer's instructions. PCR was carried out under the following conditions: a preliminary denaturation step of 5 min at 94 °C; 30 cycles of denaturation for 30 s at 94 °C, annealing for 45 s at 56 °C, and extension for 1 min at 68 °C; a final extension step for 5 min at 68 °C in a Bio-Rad T-100 thermal cycler. The amplified DNA was separated by 2% TAE agarose gel electrophoresis, stained with ethidium bromide, and visualized by UV trans-illumination in a gel documentation system (Gel Doc EZ Imager, Bio-Rad).

Enzyme-Linked Immunosorbent Assay (ELISA). Nickel substrates with or without pG-6xHis (5 μg) were incubated with anti-mouse IgG-HRP (Sigma, 1:200) in 200 μL of PBS−BSA (10 mg/mL) for 15 min. The substrate was washed 5-fold with PBS and transferred to a 96-well ELISA microplate containing 100 μL aliquots of an enhanced chemiluminescence detection solution containing 1.25 mM luminol (Sigma), 200 μM *p*-coumaric acid (Sigma), and H_2O_2 (Sigma) 0.02% (v/v) in 10 mL of 100 mM Tris-HCl (pH 8.0). After 1 min incubation in the dark, the plates were read at 490 nm using the EnVision ELISA plate reader (PerkinElmer).

Conflict of Interest: The authors declare no competing financial interest.

Acknowledgment. We thank E. Solla for SEM characterization. I. Pazos is thanked for ultramicrotome preparation. S.M. acknowledges the Action "Supporting Postdoctoral Researchers" of the Operational Program "Education and Lifelong Learning" (Action's Beneficiary: General Secretariat for Research and Technology of Greece), which is cofinanced by the European Social Fund (ESF) and the Greek State [project code PE4(1546)]. This work was supported by the European Research Council (PLASMAQUO, 267867).

Supporting Information Available: Additional transmission electron microscopy image of Ni NPs and size histogram. EDX analysis and TEM image of the Ni NP-doped substrate used in this present work. Additional XPS spectra and table containing time evolution data of the molar percentages of Ni^0 and Ni^{2+} during etching. Time course analysis of pG-6xHis release with 1 M imidazole. Additional bright field and fluorescence microscopy images of nickel substrate stained with anti-mouse IgG-FITC at various magnifications. Fluorescence microscopy images of *Salmonella* bacteria bound to a nickel NP-doped cellulose fiber imaged at various focal planes. This material is available free of charge *via* the Internet at http://pubs.acs.org.

REFERENCES AND NOTES

1. Langer, R.; Tirrell, D. A. Designing Materials for Biology and Medicine. *Nature* **2004**, *428*, 487–492.
2. Huebsch, N.; Mooney, D. J. Inspiration and Application in the Evolution of Biomaterials. *Nature* **2009**, *462*, 426–432.

3. Kim, D.; Herr, A. E. Protein Immobilization Techniques for Microfluidic Assays. *Biomicrofluidics* **2013**, *7*, 41501–41547.
4. Kong, F.; Hu, Y. F. Biomolecule Immobilization Techniques for Bioactive Paper Fabrication. *Anal. Bioanal. Chem.* **2012**, *403*, 7–13.
5. Pelton, R. Bioactive Paper Provides a Low-Cost Platform for Diagnostics. *TRAC-Trend. Anal. Chem.* **2009**, *28*, 925–942.
6. Nery, E. W.; Kubota, L. T. Sensing Approaches on Paper-Based Devices: A Review. *Anal. Bioanal. Chem.* **2013**, *405*, 7573–7595.
7. Zhao, W. A.; van den Berg, A. Lab on Paper. *Lab Chip* **2008**, *8*, 1988–1991.
8. Hussack, G.; Luo, Y.; Veldhuis, L.; Hall, J. C.; Tanha, J.; MacKenzie, R. Multivalent Anchoring and Oriented Display of Single-Domain Antibodies on Cellulose. *Sensors-Basel* **2009**, *9*, 5351–5367.
9. Costa, M. N.; Veigas, B.; Jacob, J. M.; Santos, D. S.; Gomes, J.; Baptista, P. V.; Martins, R.; Inacio, J.; Fortunato, E. A Low Cost, Safe, Disposable, Rapid and Self-Sustainable Paper-Based Platform for Diagnostic Testing: Lab-on-Paper. *Nanotechnology* **2014**, *25*, 094006.
10. Gaberc-Porekar, V.; Menart, V. Perspectives of Immobilized-Metal Affinity Chromatography. *J. Biochem. Biophys. Meth.* **2001**, *49*, 335–360.
11. Block, H.; Maertens, B.; Spriestersbach, A.; Brinker, N.; Kubicek, J.; Fabis, R.; Labahn, J.; Schafer, F. Immobilized-Metal Affinity Chromatography (IMAC): A Review. *Meth. Enzymol.* **2009**, *463*, 439–473.
12. Yang, H. M.; Liang, S. J.; Tang, J. B.; Chen, Y.; Cheng, Y. Z. Immobilization of Unraveled Immunoglobulin G Using Well-Oriented ZZ-His Protein on Functionalized Microtiter Plate for Sensitive Immunoassay. *Anal. Biochem.* **2013**, *432*, 134–138.
13. Seefeld, T. H.; Halpern, A. R.; Corn, R. M. On-Chip Synthesis of Protein Microarrays from DNA Microarrays *via* Coupled *in Vitro* Transcription and Translation for Surface Plasmon Resonance Imaging Biosensor Applications. *J. Am. Chem. Soc.* **2012**, *134*, 12358–12361.
14. Nieba, L.; Nieba-Axmann, S. E.; Persson, A.; Hamalainen, M.; Edebratt, F.; Hansson, A.; Lidholm, J.; Magnusson, K.; Karlsson, A. F.; Pluckthun, A. BIACORE Analysis of Histidine-Tagged Proteins Using a Chelating NTA Sensor Chip. *Anal. Biochem.* **1997**, *252*, 217–228.
15. Wegner, S. V.; Spatz, J. P. Cobalt(III) as a Stable and Inert Mediator Ion between NTA and His6-Tagged Proteins. *Angew. Chem., Int. Ed.* **2013**, *52*, 7593–7596.
16. Zhu, H.; Bilgin, M.; Bangham, R.; Hall, D.; Casamayor, A.; Bertone, P.; Lan, N.; Jansen, R.; Bidlingmaier, S.; Houfek, T.; *et al.* Global Analysis of Protein Activities Using Proteome Chips. *Science* **2001**, *293*, 2101–2105.
17. Nam, J. M.; Han, S. W.; Lee, K. B.; Liu, X.; Ratner, M. A.; Mirkin, C. A. Bioactive Protein Nanoarrays on Nickel Oxide Surfaces Formed by Dip-Pen Nanolithography. *Angew. Chem., Int. Ed.* **2004**, *43*, 1246–1249.
18. Lee, K. B.; Park, S.; Mirkin, C. A. Multicomponent Magnetic Nanorods for Biomolecular Separations. *Angew. Chem., Int. Ed.* **2004**, *43*, 3048–3050.
19. Lee, I. S.; Lee, N.; Park, J.; Kim, B. H.; Yi, Y. W.; Kim, T.; Kim, T. K.; Lee, I. H.; Paik, S. R.; Hyeon, T. Ni/NiO Core/Shell Nanoparticles for Selective Binding and Magnetic Separation of Histidine-Tagged Proteins. *J. Am. Chem. Soc.* **2006**, *128*, 10658–10659.
20. Kim, J.; Piao, Y.; Lee, N.; Park, Y. I.; Lee, I. H.; Lee, J. H.; Paik, S. R.; Hyeon, T. Magnetic Nanocomposite Spheres Decorated with NiO Nanoparticles for a Magnetically Recyclable Protein Separation System. *Adv. Mater.* **2010**, *22*, 57–60.
21. Sjobring, U.; Bjorck, L.; Kastern, W. Streptococcal Protein G. Gene Structure and Protein Binding Properties. *J. Biol. Chem.* **1991**, *266*, 399–405.
22. Rolland, J. P.; Mourey, D. A. Paper as a Novel Material Platform for Devices. *MRS Bull.* **2013**, *38*, 299–305.
23. Polavarapu, L.; Liz-Marzan, L. M. Towards Low-Cost Flexible Substrates for Nanoplasmonic Sensing. *Phys. Chem. Chem. Phys.* **2013**, *15*, 5288–5300.
24. Mourdikoudis, S.; Liz-Marzan, L. M. Oleylamine in Nanoparticle Synthesis. *Chem. Mater.* **2013**, *25*, 1465–1476.
25. Sanchez-Iglesias, A.; Grzelczak, M.; Perez-Juste, J.; Liz-Marzan, L. M. Binary Self-Assembly of Gold Nanowires with Nanospheres and Nanorods. *Angew. Chem., Int. Ed.* **2010**, *49*, 9985–9989.
26. Dong, A.; Chen, J.; Vora, P. M.; Kikkawa, J. M.; Murray C. B. Binary Nanocrystal Superlattice Membranes Self-Assembled at the Liquid-Air Interface. *Nature* **2010**, *466*, 474–477.
27. Donegan, K. P.; Godsell, J. F.; Otway, D. J.; Morris, M. A.; Roy, S.; Holmes, J. D. Size-Tuneable Synthesis of Nickel Nanoparticles. *J. Nanopart. Res.* **2012**, *14*, 670(1−10).
28. Hasan, S. A.; Kavich, D. W.; Dickerson, J. H. Sacrificial Layer Electrophoretic Deposition of Free-Standing Multilayered Nanoparticle Films. *Chem. Commun.* **2009**, 3723–3725.
29. Moulder, J. F.; Stickle, W. F.; Sobol, P. E.; Bomben, K. D. *Handbook of X Ray Photoelectron Spectroscopy: A Reference Book of Standard Spectra for Identification and Interpretation of XPS Data*; Physical Electronics: MN, 1995; Vol. 86.
30. Getz, E. B.; Xiao, M.; Chakrabarty, T.; Cooke, R.; Selvin, P. R. A Comparison between the Sulfhydryl Reductants Tris (2-carboxyethyl)phosphine and Dithiothreitol for Use in Protein Biochemistry. *Anal. Biochem.* **1999**, *273*, 73–80.
31. Guss, B.; Eliasson, M.; Olsson, A.; Uhlen, M.; Frej, A. K.; Jornvall, H.; Flock, J. I.; Lindberg, M. Structure of the Igg-Binding Regions of Streptococcal Protein-G. *EMBO J.* **1986**, *5*, 1567–1575.
32. Lee, J. M.; Park, H. K.; Jung, Y.; Kim, J. K.; Jung, S. O.; Chung, B. H. Direct Immobilization of Protein G Variants with Various Numbers of Cysteine Residues on a Gold Surface. *Anal. Chem.* **2007**, *79*, 2680–2687.
33. Hendriksen, R. S.; Vieira, A. R.; Karlsmose, S.; Wong, D. M. A. L. F.; Jensen, A. B.; Wegener, H. C.; Aarestrup, F. M. Global Monitoring of *Salmonella* Serovar Distribution from the World Health Organization Global Foodborne Infections Network Country Data Bank: Results of Quality Assured Laboratories from 2001 to 2007. *Foodborne Pathog. Dis.* **2011**, *8*, 887–900.
34. Choudhary, S.; Schmidt-Dannert, C. Applications of Quorum Sensing in Biotechnology. *Appl. Microbiol. Biotechnol.* **2010**, *86*, 1267–1279.
35. Shin, H. J. Genetically Engineered Microbial Biosensors for *in Situ* Monitoring of Environmental Pollution. *Appl. Microbiol. Biotechnol.* **2011**, *89*, 867–877.
36. Liu, Y.; Rafailovich, M. H.; Malal, R.; Cohn, D.; Chidambaram, D. Engineering of Bio-Hybrid Materials by Electrospinning Polymer-Microbe Fibers. *Proc. Natl. Acad. Sci. U.S.A.* **2009**, *106*, 14201–14206.
37. Weile, J.; Knabbe, C. Current Applications and Future Trends of Molecular Diagnostics in Clinical Bacteriology. *Anal. Bioanal. Chem.* **2009**, *394*, 731–742.
38. Fredricks, D. N.; Relman, D. A. Improved Amplification of Microbial DNA from Blood Cultures by Removal of the PCR Inhibitor Sodium Polyanetholesulfonate. *J. Clin. Microbiol.* **1998**, *36*, 2810–2816.
39. Handschur, M.; Karlic, H.; Hertel, C.; Pfeilstocker, M.; Haslberger, A. G. Preanalytic Removal of Human DNA Eliminates False Signals in General 16S rDNA PCR Monitoring of Bacterial Pathogens in Blood. *Comp. Immunol. Microbiol.* **2009**, *32*, 207–219.
40. Rozhok, S.; Fan, Z. F.; Nyamjav, D.; Liu, C.; Mirkin, C. A.; Holz, R. C. Attachment of Motile Bacterial Cells to Prealigned Holed Microarrays. *Langmuir* **2006**, *22*, 11251–11254.
41. Rowan, B.; Wheeler, M. A.; Crooks, R. M. Patterning Bacteria within Hyperbranched Polymer Film Templates. *Langmuir* **2002**, *18*, 9914–9917.
42. Premkumar, J. R.; Lev, O.; Marks, R. S.; Polyak, B.; Rosen, R.; Belkin, S. Antibody-Based Immobilization of Bioluminescent Bacterial Sensor Cells. *Talanta* **2001**, *55*, 1029–1038.
43. Suo, Z. Y.; Avci, R.; Yang, X. H.; Pascual, D. W. Efficient Immobilization and Patterning of Live Bacterial Cells. *Langmuir* **2008**, *24*, 4161–4167.
44. Chiu, C. H.; Ou, J. T. Rapid Identification of *Salmonella* Serovars in Feces by Specific Detection of Virulence Genes, invA and spvC, by an Enrichment Broth Culture-Multiplex PCR Combination Assay. *J. Clin. Microbiol.* **1996**, *34*, 2619–2622.

45. Malorny, B.; Hoorfar, J.; Bunge, C.; Helmuth, R. Multicenter Validation of the Analytical Accuracy of *Salmonella* PCR: Towards an International Standard. *Appl. Environ. Microbiol.* **2003**, *69*, 290–296.
46. Sheldon, R. A.; van Pelt, S. Enzyme Immobilisation in Biocatalysis: Why, What and How. *Chem. Soc. Rev.* **2013**, *42*, 6223–6235.
47. Liese, A.; Hilterhaus, L. Evaluation of Immobilized Enzymes for Industrial Applications. *Chem. Soc. Rev.* **2013**, *42*, 6236–6249.